ULTRASONIC INDICATION SIZING TECHNIQUE DEVELOPMENT

DRAFT FINAL REPORT
SwRI Project 2388

Prepared for

Rochester Gas & Electric Corporation
89 East Avenue
Rochester, New York 14649

Wisconsin Electric Power Company
6610 Nuclear Road
Two Rivers, Wisconsin 54241

Prepared by

Nondestructive Evaluation Science and Technology Division

February 1989

TABLE OF CONTENTS

I. INTRODUCTION

Ultrasonic examinations to locate and size flaws in the nozzle-to-shell welds in reactor pressure vessels (RPV) have long been performed by positioning the transducers on the inner bore of the nozzles. These examinations have been very satisfactory for detecting flaws and for locating small fabrication-induced indications parallel to the fusion line of the weld. Some problems have become apparent, however, when attempting to size the flaws using transducers similar to those applied for detection. Problems include the inability to locate the end points in both the circumferential and through-wall (axial) directions accurately enough to estimate, respectively, the length and depth of planar flaws in the weld. It is believed that the cylindrical or in some cases conical bores of the nozzles distort the beam, which complicates accurate sizing. One technique for sizing flaws in the nozzle-bore region has been to perform a type of beam focusing by removing the transducer beam spread from the actual sizing measurement. The intent has been to attain a more conservative and accurate flaw length and depth estimate.

Beam-spread sizing techniques have been used since 1976 to size flaws during nozzle-bore examinations at both the Point Beach and R. E. Ginna nuclear plants. While this approach was considered adequate, it was recognized that several recently developed and well documented flaw-sizing techniques had proven to be quite accurate in various tests such as the PISC trials. These techniques also had been applied successfully in other types of field examinations.

Because of the availability of the new flaw-sizing techniques, a project was initiated at Southwest Research Institute (SwRI) in August 1988 by Wisconsin Electric Power Company and Rochester Gas & Electric Corporation to evaluate two of these techniques. The purpose was to develop their applicability for addressing the nozzle-bore flaw-sizing problems encountered at Point Beach and R. E. Ginna. The project consisted of building mockups of the specific geometries involved, placing planar reflectors at the location of the fusion line of the nozzle-to-vessel welds (where indications

had been previously located), and performing flaw-sizing exercises with newly developed transducer-technique combinations to prove the adequacy of the selected approaches. Finally, the flaw-sizing data acquired using the new procedures was to be compared with flaw-sizing data acquired from performing conventional examinations on the nozzle mockups following ASME Code procedures (see Figure 1). The two special procedures chosen for this project used (1) large-diameter focused transducers with amplitude-drop sizing techniques (Figure 2) and (2) conventional transducers with time-of-flight techniques for detecting the diffracted signals from the sharp ends of the planar flaws in both the through-wall (depth) and circumferential (length) directions (Figure 3).

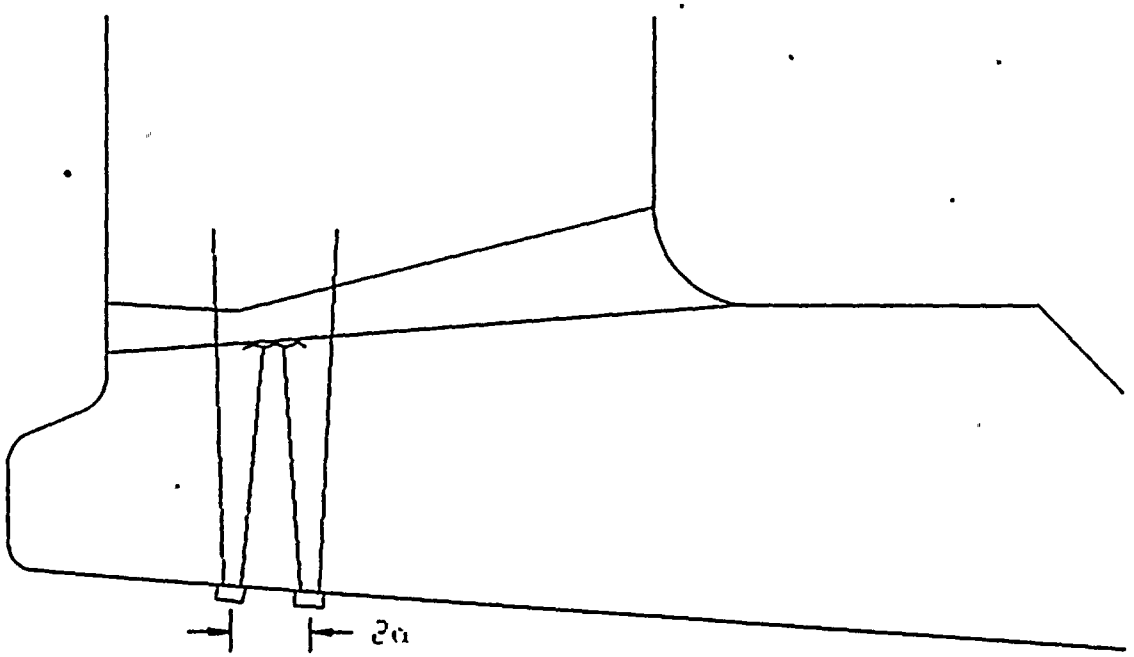

Figure 1. Straight-beam, unfocused transducer approach (Code-sizing technology)

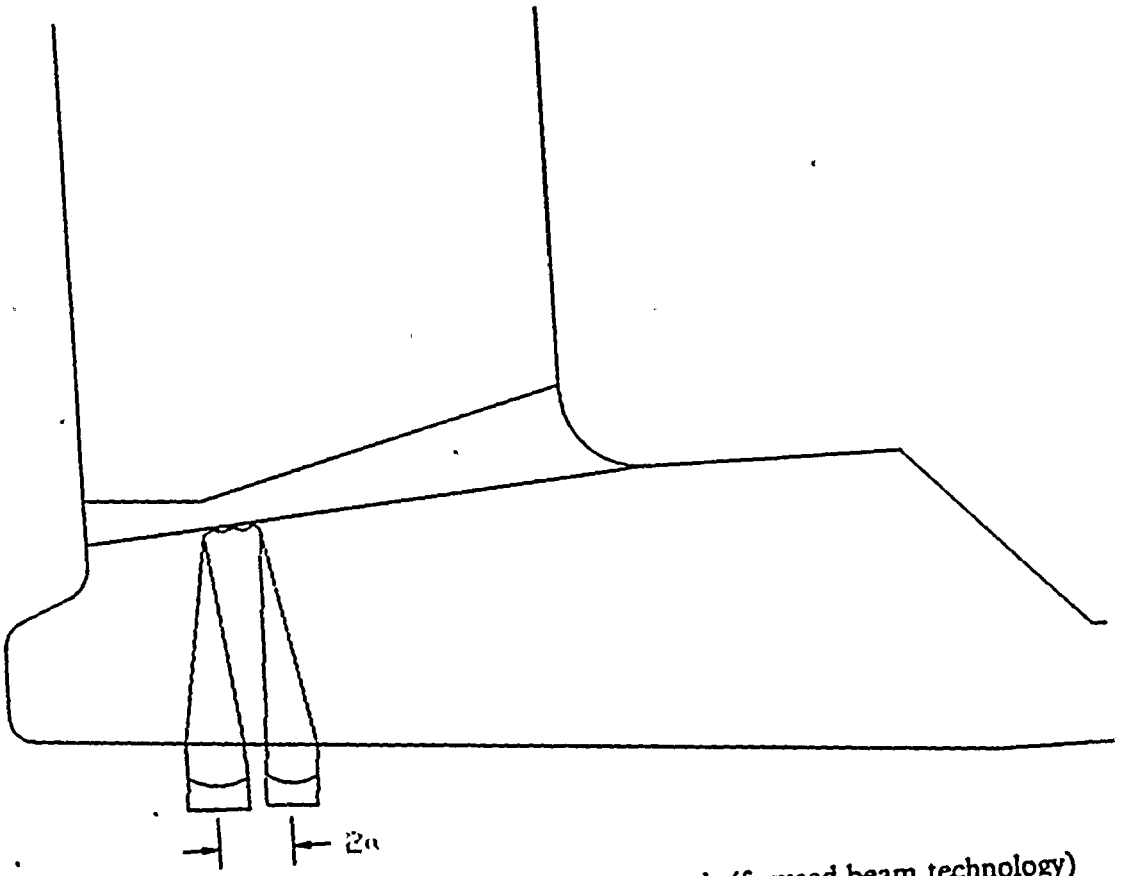

Figure 2. Straight-beam, focused transducer approach (focused-beam technology)

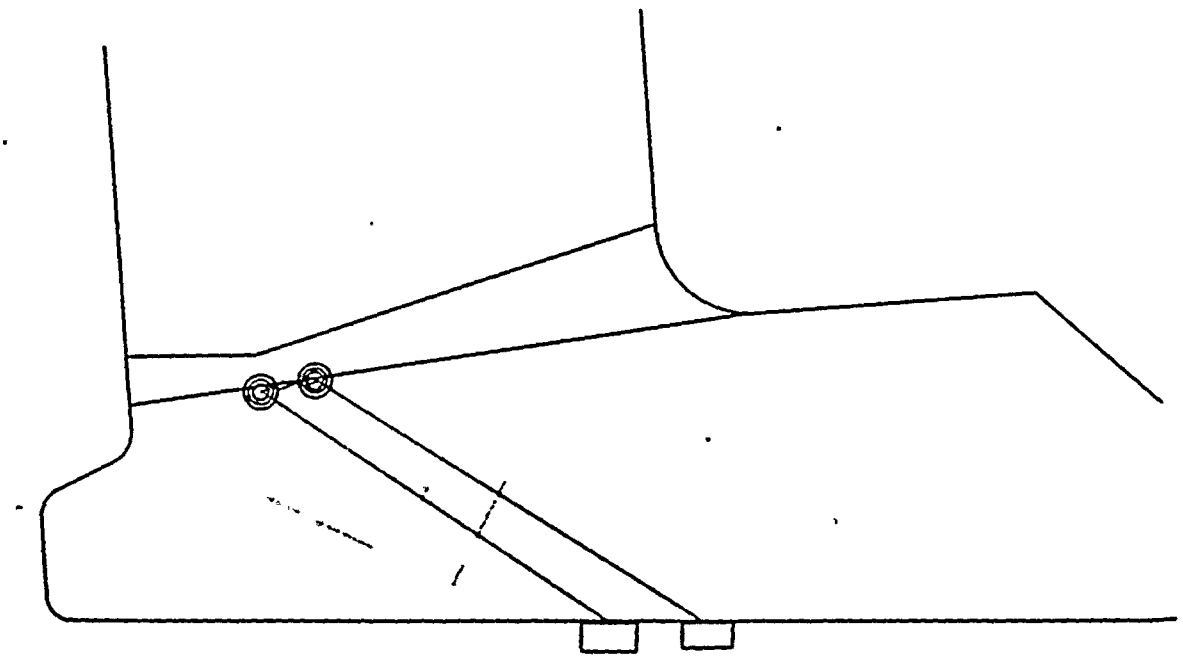

Figure 3. Angle-beam, unfocused transducer approach (time-of-flight technology)

II. BACKGROUND

The transducer-technique combinations chosen for evaluation have been well documented in recent studies by the Electric Power Research Institute and other organizations engaged in ultrasonic examination research and development. The focused beam technology has been used for a number of years by an examination agency in France to size small flaws in the nozzle-to-shell weld region as well as elsewhere in the reactor vessel wall. Variations of the time-of-flight technology have been applied by a number of agencies in Europe, the Orient, and the United States. SwRI has a significant amount of experience in time-of-flight flaw identification and sizing techniques, many of which have been developed by Dr. George J. Gruber.

III. TECHNICAL DISCUSSION

A. Introduction

The scope of this project was to develop flaw-sizing techniques to be used in the two nozzle configurations present in the Point Beach and R. E. Ginna RPVs. One mockup configuration simulated the inlet/outlet nozzles; the other the core-flood, or safety-injection, nozzles. The inlet/outlet nozzle, with a conical bore diameter of approximately 30 inches, was cladded with stainless steel and then hand ground to a relatively smooth finish. The core-flood nozzle, with a 3.4-inch diameter bore, was also cladded with stainless steel, but was machined smooth. These two geometries represented significantly different problems that had to be addressed in order to direct and control the ultrasonic beams at the areas of interest.

B. Inspection Techniques

The focused-beam flaw-sizing technology employed large-diameter transducers to focus the ultrasonic beam to as small a point as practical at the specific depth locations of the reflectors. The focused beam was moved across each reflector utilizing an amplitude-drop technique to define the reflector edges. Because the beam diameter at the reflector location was small relative to the size of each reflector, the ability to accurately define and locate the edges of the reflector was significantly enhanced. To do this, the bore configuration of both nozzles had to be carefully taken into consideration in the design of the transducer lenses so that proper focusing could take place in the material. An additional consideration was the plane of the reflector, which is typically oriented several degrees off normal from the nozzle bore. Once the lens was designed, it was just as important to assure that the mechanical scanning equipment could position the transducer accurately relative to the bore of the nozzle so that the sound beam was focused properly in the test material.

The time-of-flight flaw-sizing technology was based upon the selection of conventional transducers; no attempt was made to focus the ultrasonic beam. The approach was to introduce the sound beam obliquely to the reflector so that the strong specularly reflected waves--which can mask the real tip-diffracted waves--were not returned to the transducer. This approach allowed observance of the diffracted signals from all four edges of a planar reflector. Accurate screen-distance calibration permitted the measurement of the times that it took for a pair of diffracted signals (doublet) to reach an axially (or circumferentially) scanned transducer. Simple ray-tracing calculations were performed that considered the sound-beam angle and the relationship between the difference in time-of-flight of the two tip-diffracted signals (doublet separation as defined in the satellite-pulse observation technique) and the reflector depth (or length). The result was an accurate estimate of the through-wall dimension (or length) of the reflector depending on which

diffracted signal pair was being produced. The amplitude-drop technique was applied to the C-scan data using the time-of-flight technology to estimate flaw length.

While it was recognized that readily detectable tip-diffracted waves are not necessarily generated from real flaws in every case to provide time-of-flight flaw-sizing information, it was anticipated that using a combination of the focused transducer and time-of-flight techniques would provide accurate sizing of the planar flaws in question.

C. Test Mockups

In order to adequately test and qualify these two special approaches, it was necessary to build realistic mockups of the nozzle geometries in question. It was determined that two mockups would be fabricated, one representing the inlet/outlet nozzle configuration and the other, the core-flood, or safety-injection, nozzle. These mockups were fabricated from forged material similar to that used in the actual nozzles of the RPV. A 90-degree section mockup of the inlet/outlet nozzle (Figure 4) and a full 360-degree core-flood nozzle mockup (Figure 5) were built. Six planar flaws were placed in the inlet/outlet mockup, and five planar flaws, in the core-flood mockup (see Table 1). The flaws consisted of machined notches and flat-bottom holes placed at locations representing the nozzle-to-shell weld fusion line nearest the nozzle bore. The planar flaws were chosen because these most accurately represented the flaws detected in the nozzle-to-shell welds in question and other excavated and confirmed nozzle fabrication flaws. (See Appendix A for a discussion about the nozzle-to-shell weld flaws.)

Flaw sizes ranged from 1 percent t (through-wall thickness) (0.094 inch) in the through-wall dimension of the RPV weld by approximately 1/2 inch in length, to 12 percent t (1.093 inches in diameter) in the through-wall dimension (flat-bottom hole). In each mockup, two small notches

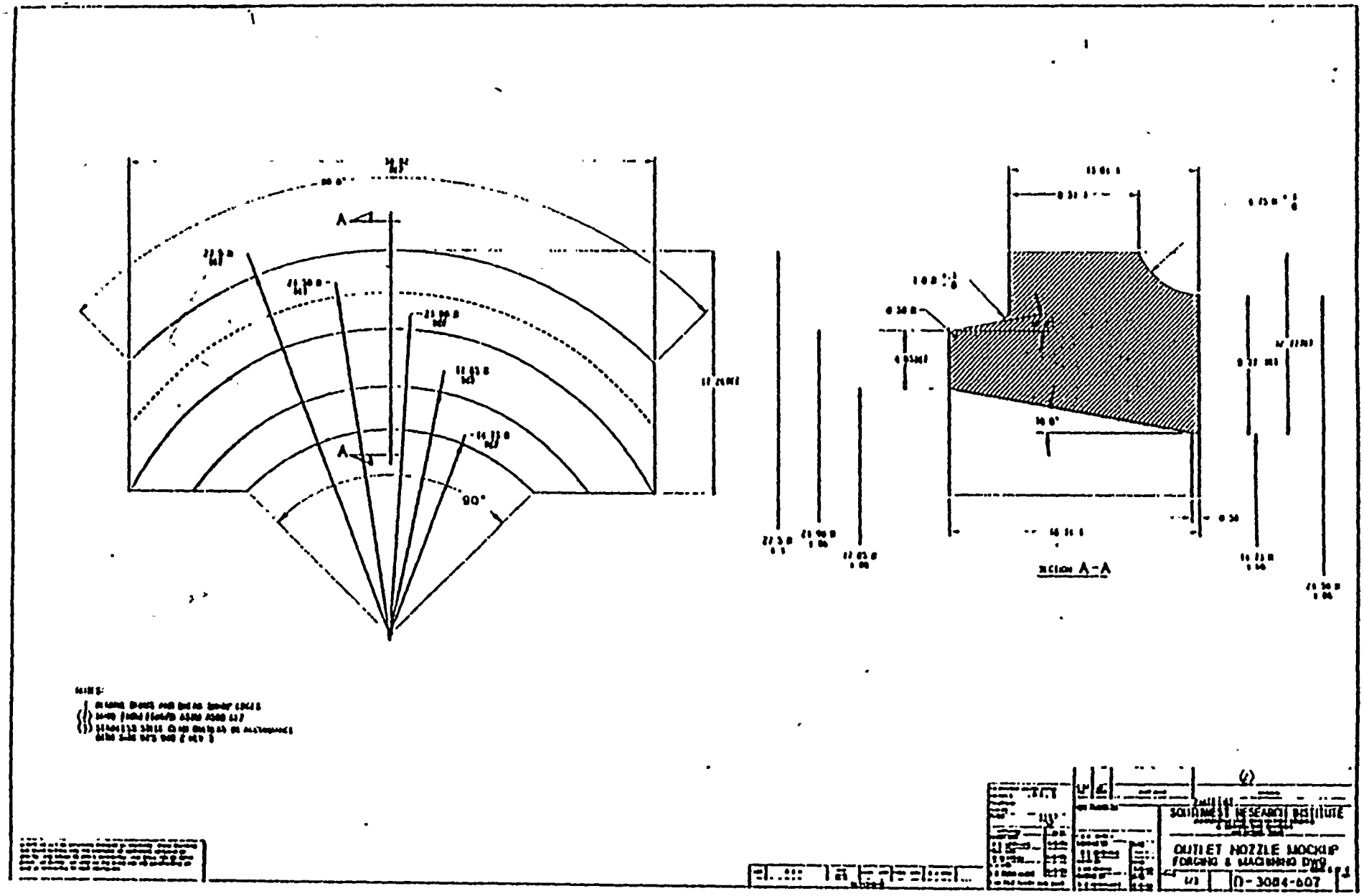

Figure 4. Inlet/outlet nozzle mockup

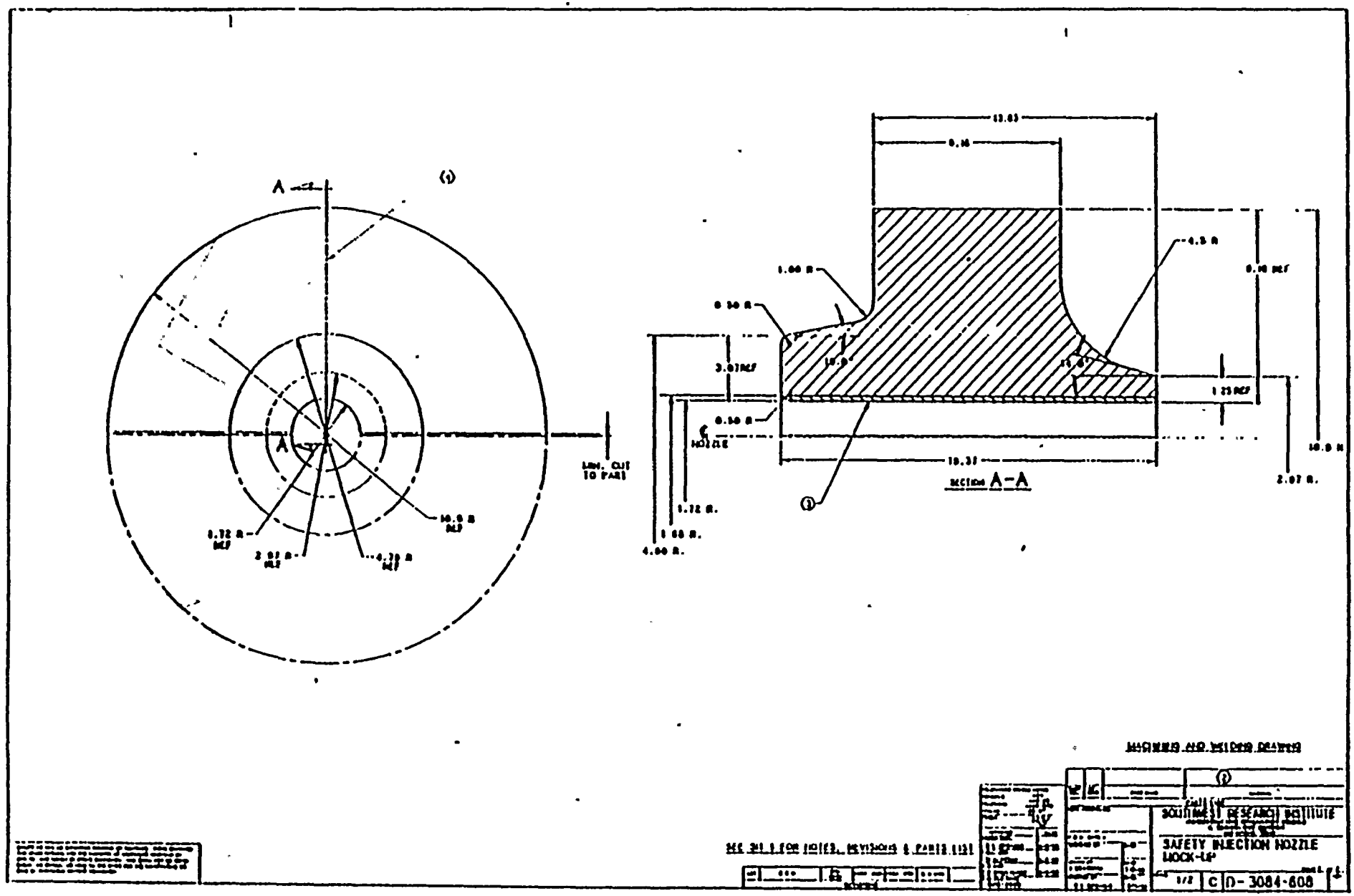

Figure 5. Core-flood, or safety-injection, nozzle mockup

Table 1

SIZE OF REFLECTOR MACHINED INTO THE CORE-FLOOD AND INLET/OUTLET MOCKUPS
(measured to the nearest thousandth of an inch)

Core-Flood Mockup Reflectors: Length x Depth (in.)	Inlet/Outlet Mockup Reflectors: Length x Depth (in.)
0.188 x 1.00	0.094 x 0.500
0.188 x 0.500 (two reflectors)	0.188 x 0.500
0.562 x 1.093	0.188 x 0.500 (two reflectors)
1.093 dia. round flat-bottom hole	0.562 x 1.093
	1.093 dia. flat-bottom hole

(twin flaws) were placed in close proximity to determine the ability of the applied transducer-technique combinations to separate the individual flaws.

D. Technique Evaluation

Once the techniques were chosen and the transducers and mockups built, a comprehensive scanning program was performed using field examination and positioning equipment as well as field recording equipment to perform the flaw-sizing exercises. The mockups were placed in the SwRI scanning tank (used for the uncontaminated PaR Device), and several sets of scans were made on each mockup flaw. The scan data were recorded and analyzed on the SwRI EDAS color-imaging ultrasonic system, and the size estimates for each flaw were compared to the actual sizes of the flaws in the mockups.

Several different focused-beam transducers were used on both the inlet/outlet and the core-flood nozzle mockups to determine the best transducers. Based upon these studies, focused transducers were chosen for each type of nozzle. The optimum inlet/outlet nozzle transducer was a 3-

by 3-inch piezoelectric crystal that focused in both the axial and circumferential directions. The optimum core-flood nozzle transducer, which also focused in both the axial and circumferential directions, contained a 1- by 3-inch piezoelectric crystal. The frequency of both transducers was 5 MHz.

Identical search-unit module designs (a 35-degree longitudinal-wave search unit for axial scanning and flaw-depth estimation and a 45-degree longitudinal-wave search unit for circumferential scanning and flaw-length estimation) were adopted for both nozzles by the time-of-flight technology. The frequency of both transducers was 5 MHz.

In order to compare the special sizing procedures with the beam-spread sizing procedure (ASME technology) used in the past, it was necessary to perform scanning with standard detection transducers and size the flaws.

The actual flaw sizes and the size estimates obtained using the three different flaw-sizing technologies are shown in Tables 2 and 3.

Table 2

DEPTH X LENGTH ESTIMATES (IN.) OBTAINED BY THE ASME CODE, FOCUSED-BEAM, AND TIME-OF-FLIGHT PROCEDURES FOR THE FIVE CORE-FLOOD, OR SAFETY-INJECTION, NOZZLE FLAWS

Actual Flaw Size (in.)	Size Estimates		
	ASME Code (in.)	Focused Beam (in.)	Time of Flight (in.)
0.19 x 0.50	0.44 x 1.15	0.28 x 0.79	0.20 x 0.75
0.19 x 0.50	0.36 x 1.15	0.28 x 0.79	0.20 x 0.35
0.19 x 1.00	0.69 x 2.30	0.32 x 1.07	0.25 x 1.20
0.56 x 1.09	1.05 x 2.55	0.60 x 1.21	0.55 x 0.95
1.09 round	1.05 x 2.55	1.08 x 1.36	1.10 x 1.20

Table 3

DEPTH X LENGTH ESTIMATES (IN.) OBTAINED BY THE ASME CODE, FOCUSED-BEAM, AND TIME-OF-FLIGHT PROCEDURES FOR THE SIX INLET/OUTLET NOZZLE FLAWS

Actual Flaw Size (in.)	Size Estimates		
	ASME Code (in.)	Focused Beam (in.)	Time of Flight (in.)
0.09 x 0.50	0.38 x 1.21	0.36 x 0.55	0.10 x 0.65
0.19 x 0.50	1.66 x 2.11	0.32 x 0.48	0.20 x 0.45
0.19 x 0.50	------	0.40 x 0.48	0.20 x 0.55
0.19 x 1.00	1.18 x 2.22	0.50 x 1.20	0.20 x 0.95
0.56 x 1.09	2.05 x 2.44	0.64 x 1.10	0.60 x 1.20
1.09 round	2.56 x 2.55	1.60 x 1.24	1.15 x 1.20

E. Procedure Development

Once the flaw-sizing data were analyzed, the transducers and the techniques were incorporated into special field procedures to be used for flaw sizing during the upcoming R. E. Ginna RPV examination.

F. Evaluation of the Framatome Focused Search Units

Two Framatome focused search units were delivered to SwRI for possible evaluation on the inlet/outlet and core-flood nozzles. One unit with a 2-MHz transducer was not evaluated due to an inherent design problem and time constraints on the PaR Device. The search unit was constructed with a plastic sheath holding the various elements together. It was determined that the plastic sheath must be replaced by a metal one to ensure structural integrity. The second Framatome search unit, with a 4-inch diameter and 2.4-MHz frequency transducer, was tested on the inlet/outlet nozzle. The transducer was operated at the design conditions of a 4-inch standoff distance at 15 degrees. The results of the EDAS data analysis showed greatly oversized defects.

For example, the data on the 0.562 by 1.093-inch notch showed that at 10 percent (or 20 dB down), the estimated size was 0.88 by 6.52 inches; at 25 percent (or 12 dB down), estimated size was 0.68 by 4.96 inches; at 50 percent (or 6 dB down), estimated size was 0.44 by 2.59 inches. Data on the other notches illustrated similar oversizing. The problem appeared to be related to the frequency of the transducer, since the 2.25-MHz focused data acquired during this project compared with the 5-MHz focused data showed similar overestimation of the defect size.

IV. RESULTS

As evidenced by the data in Tables 2 and 3, flaw sizing using both special procedures produced extremely good results. The amplitude-drop point chosen for focused-beam sizing was 25 percent of maximum signal amplitude; it was chosen specially for the purpose of yielding slightly conservative results. The data showed that with this 12-dB drop sizing criterion, none of the flaws in the two mockups were undersized. For the core-flood mockup flaws, the maximum oversizing in through-wall dimension was 0.13 inch. For the inlet/outlet nozzle mockup flaws, the maximum oversizing in through-wall dimension was 0.5 inch. The mean errors of overestimation for the core-flood and inlet/outlet nozzle mockup flaws were 0.1 inch and 0.2 inch, respectively. Length measurements were within 0.3 inch of actual length.

The satellite-pulse observation technique of the time-of-flight technology was applied to the B-scan data obtained for the eleven mockup flaws with the axially scanned transducers to estimate flaw depth. Maximum oversizing in the through-wall dimension was 0.1 inch. The amplitude-drop technique of the time-of-flight technology was applied to the C-scan data obtained for the eleven mockup flaws to estimate their length. The length estimates were within 0.25 inch of their actual values (90-percent confidence level).

V. CONCLUSIONS

The project was very successful. In every case, the focused-beam and time-of-flight techniques yielded much more accurate sizing results than those obtained using the Code techniques. It is anticipated that with the completion of the project and qualification of the new technologies, the disposition of flaw indications of this nature will be much more straightforward and acceptable to the regulatory bodies in future examinations. The proceduralization of the employed transducer-technique combinations and available imaging equipment will also assure that the sizing of planar flaws will be more clearly defined in the documentation.

ATTACHMENT 5

STRUCTURAL INTEGRITY LETTER

STRUCTURAL INTEGRITY ASSOCIATES, INC.

3[illegible] Almaden Expressway
Suite 226
San Jose, CA 95118
(408) 978-8200
TELEX: 184817 STRUCT
FAX: (408) 978-8964

Fossil Plant Operations
66 South Miller Road
Suite 10
Akron, Ohio 44313
(216) 864-8886
FAX: (216) 869-5461

April 26, 1989
JFC-89-034
SIR-89-026, Rev. 0

Michael J. Saporito
Rochester Gas & Electric Corp.
R. E. Ginna Nuclear Power Station
1503 Lake Road
Ontario, NY 14519

Subject: ASME Code Section XI Acceptability of the "B" Inlet Nozzle Flaw Indication in the R.E. Ginna Reactor Vessel, Based on Spring 1989 Inservice Inspection Results

Dear Mike:

The subject inservice inspection (ISI) flaw indication has been evaluated by us as acceptable in accordance with ASME Section XI for continued service without repair, as shown on the attached calculation package sheets. Since the flaw, interpreted as an original construction slag defect at approximately midwall of the nozzle-to-vessel weld, is shown by the present UT examination to be smaller than when it was evaluated as acceptable by Teledyne in 1979, that earlier report conservatively bounds the current flaw evaluation.

In summary, our attached flaw evaluation supports the following conclusions:

1. Irradiation effects from the core are negligible at the flaw location,

2. The applied fracture mechanics K for the embedded flaw with a through-wall dimension of 0.48 inches and a length of 4.94 inches is calculated as 7351 psi.$\sqrt{\text{in.}}$ due to the pressure loading and weld residual stresses described in the Teledyne report,

3. The above K provides a margin of 27.2 against an upper shelf reference K (K_{IR}) of 200,000 psi.$\sqrt{\text{in.}}$, compared to a Section XI required margin of 3.16, and

4. Predicted fatigue crack growth, verified by the ISI experience, is negligible.

Please let me know if you require further information.

Very truly yours,

Fred Copeland

J.F. Copeland
Associate

Reviewed by:

S. S. Tang

/mc
attachment

cc: John F. Smith

ATTACHMENT 6

STRUCTURAL INTEGRITY ANALYSIS

RGE-04Q

CALCULATION PACKAGE

GINNA B INLET NOZZLE ISI INDICATION

OBJECTIVE:

Evaluate the subject indication for acceptability per ASME Section XI [1].

FLAW SIZE AND LOCATION: [2-5]

Embedded construction defect (slag). The location in the nozzle weld is shown [2-4] below and in the attached CAD drawing [5].

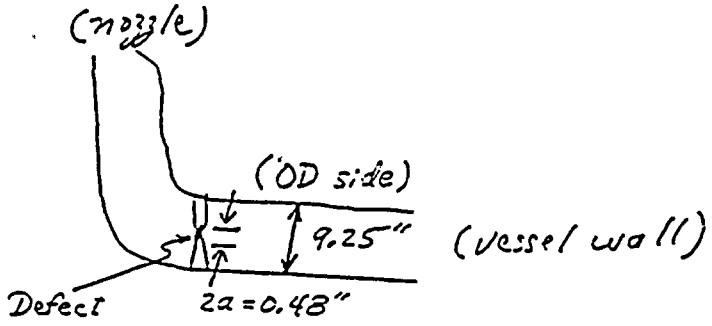

ℓ = 4.94" (into paper)
t = 9.25" (at indication location)
e < = 0.625" (on OD side of mid-wall)

a/ℓ = 0.24/4.94 = 0.049
2a/t = 0.48/9.25 = 0.052
2e/t = 1.25/9.25 = 0.135

STRESSES:

From the 1979 Teledyne report [6],

σ_m = 6,733 psi
$\sigma_b = \sigma_{residual}$ = 8,000 psi.

Prepared by: J.F. Gorman 4-26-89
Checked by: [illegible] 4/26/89
File No. RGE-04Q-300
Page 1 of 13

K CALCULATION:

See attached App. A. (Sct. XI) sheets for applicable curves.

$$K_I = \sigma_m M_m \sqrt{\pi a/Q} + \sigma_b M_b \sqrt{\pi a/Q}$$

$$= (\sigma_m M_m + \sigma_b M_b) \sqrt{\pi a/Q}$$

Conservatively take σ_{ys} = 42 ksi, as in Teledyne report [6]

$$\frac{\sigma_m + \sigma_b}{\sigma_{ys}} = \frac{6,733 + 8,000}{42,000} = 0.35$$

For the above value and $a/\ell = 0.049$, from Figure A-3300-1,

$Q = 1.02$

From Figure A-3300-2, for $2a/t = 0.052$ and $2e/t = 0.135$,

$M_m = 1.02$

From Figure A-3300-4, for the same flaw dimensions,

$M_b = 0.21$

$$\therefore K_I = [(6,733)(1.02) + (8,000)\ (0.21)] \sqrt{\pi \frac{(0.24)}{(1.02)}}$$

$$= [6,868 + 1,680]\ (0.86)$$

$$= \boxed{7351 \text{ psi} \sqrt{\text{in.}}} \quad \text{(Applied value)}$$

MATERIAL K (K_{IR}):

From WCAP-8503 [7], the outlet (and inlet) nozzles are located ~25" above the top level of the core assembly. Also in that document, the % of peak fluence at that location is about 2%. Since the ISI indication is at the 10:30 location:

Prepared by: J.F. [signature] 4-26-89
Checked by: [signature] 4/26/89
File No. RGE-04Q-300

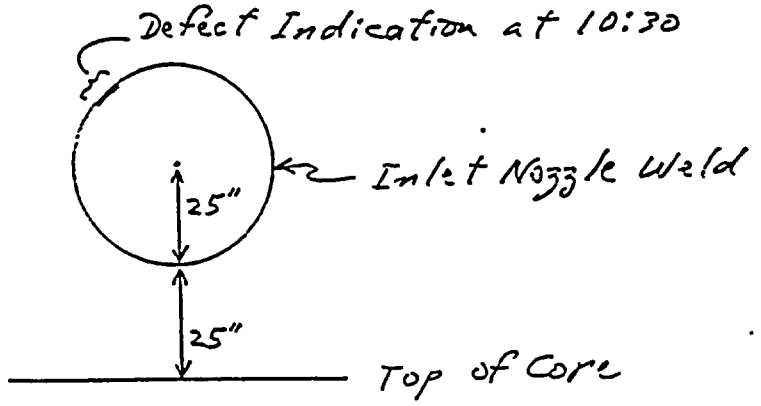

and the radius from the nozzle centerline to the defect location is 25" (Teledyne report), at least an additional 25" can be added to the above 25" number to place the defect at least 50" above the top of the core. It was verified [3] that the defect is, in fact, 57" above the core assembly. From Figure 2-3 (attached) [8], it can be seen that this gives a multiplying factor of less than 10^{-3} times the peak fluence. From the latest Ginna surveillance report (WCAP-10086) [8], the peak measured fluence at the vessel inner surface is 4.03×10^{19} n/cm^2 for 32 EFPYs. Thus, the End-of-Life fluence at the defect location is conservatively established as:

$$(4.03 \times 10^{19} \text{ n/cm}^2) \times 10^{-3}$$

$$= \boxed{4.03 \times 10^{16} \text{ n/cm}^2}$$

That value of fluence is below the threshold for consideration of degradation of toughness by irradiation damage, in accordance with 10CFR50, App. H. (No surveillance, etc. is required for locations with EOL fluence less than 10^{17} n/cm^2. Note that the ISI defect is at about mid-wall, and would see even less fluence.

Thus, the upper shelf K_{IR} value of 200 ksi $\sqrt{\text{in.}}$ used in the 1979 Teledyne report and in WCAP-8503 is still appropriate, since the beltline P-T limits assure that the inlet nozzle will be on the upper shelf, as stated in the Teledyne report.

$$K_{IR} = 200{,}000 \text{ psi } \sqrt{\text{in}}$$

for the inlet nozzle

FATIGUE CRACK GROWTH

The fatigue crack growth law for subsurface cracks, from ASME Section XI, is:

$$\frac{da}{dN} = 0.0267 \times 10^{-9} \ \Delta K^{3.726}$$

where da/dN is in./cycles and ΔK is in ksi $\sqrt{\text{in}}$.

From prior calculations in this package, the ΔK_I due to going from 0 to 2500 psig is:

$$K_{I,m} = \Delta K = 0.86 \ (6{,}868)$$
$$= 5907 \text{ psi } \sqrt{\text{in}}.$$

Substituting this ΔK into an equation to account for mean stress due to the residual stress gives:

$$K_{effective} = \Delta K/(1-R)^m$$

where: $m = 0.5$

$R = K_{min}/K_{max}$
$= 1444/7351$
$= 0.2$

$\therefore K_{effective} = 5907/(1-0.2)^{0.5}$

$= 6604 \text{ psi } \sqrt{\text{in}}. = 6.604 \text{ ksi } \sqrt{\text{in}}.$

Substituting $K_{effective}$ into the da/dN law to gain an estimate of crack growth rate gives:

$$da/dN = 2.67 \times 10^{-11} (K_{effective})^{3.726}$$

$$= 3.03 \times 10^{-8} \text{ in/cycle}$$

Even assuming 1200 full pressure cycles (0 to 2500 psig) in the 40 year life of the plant (30/yr.), which is conservative, as shown on the attached tables of transients [7,9], the predicted crack growth for 1200 cycles is insignificant:

$$\Delta a = (1200)(3.03 \times 10^{-8})$$

$$\boxed{3.6 \times 10^{-5} \text{ in.}}$$

The above value is not enough to change the value of ΔK and the crack growth rate is relatively constant and insignificant.

As mentioned in the Teledyne report [6], thermal stresses at this mid-wall location are expected to be insignificant.

CODE SAFETY FACTORS:

The Code (Sct. XI) requires a safety factor of

$$\frac{K_{IR}}{K_I} = \sqrt{10} = 3.16$$

The actual safety factor in this case is

$$\frac{K_{IR}}{K_I} = \frac{200,000}{7,351} = \boxed{27.2}$$

CONCLUSION:

The subject ISI indication is acceptable in accordance with ASME Section XI. No repair is necessary. Since the indication is currently shown as smaller in 1989 than it was in 1979, the 1979 analysis and report submitted to the NRC conservatively envelopes the evaluation of this indication.

Prepared by: J.E. [illegible] 4-26-89
Checked by: [illegible] 4/26/89
File No. RGE-040L-300

REFERENCES:

1. ASME Code, Section XI, 1983 edition or 1986 edition.

2. Telecopy, M. Saporito (RG&E) to J. F. Copeland (SI), 4-6-89.

3. Letter J. F. Smith (RG&E) to J. F. Copeland (SI), 4-11-89.

4. Letter, J. F. Smith (RG&E) to J. F. Copeland (SI), 4-12-89

5. CAD Drawing of Ginna Inlet N2B Nozzle Weld Showing ISI Indication Location, J. F. Smith (RG&E) to J. F. Copeland (SI), 4-23-89.

6. "ASME Section XI Fracture Mechanics Evaluation of Inlet Nozzle Inservice Inspection Indication," Teledyne Technical Report No. TR-3454-1, R.E. Ginna Unit No. 1 Reactor Vessel, March 15, 1979.

7. W. K. Ma, "ASME III, Appendix G Analysis of the Rochester Gas & Electric Corporation, R. E. Ginna Unit No. 1 Reactor Vessel", Westinghouse WCAP-8503, July, 1975.

8. S. E. Yanichko, et al, "Analysis of Capsule T from the Rochester Gas and Electric Corporation R. E. Ginna Nuclear Plant Reactor Vessel Radiation Surveillance Program", Westinghouse WCAP-10086, April 1982.

9. "Thermal Transients and Categories," Ginna Nuclear Power Plant, Appendix H, RG&E, July 15, 1975.

R.E. GINNA
Inlet N2B Nozzle

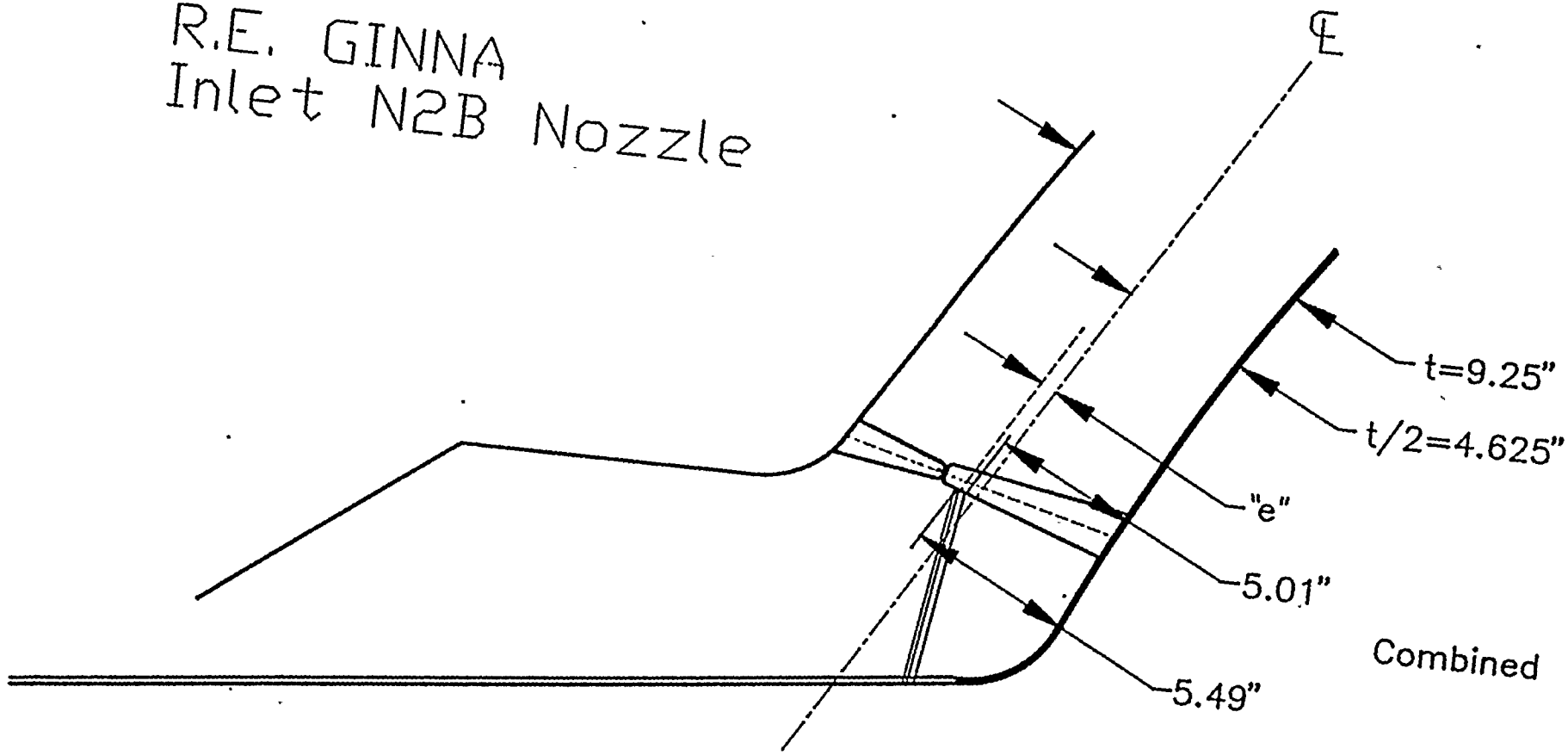

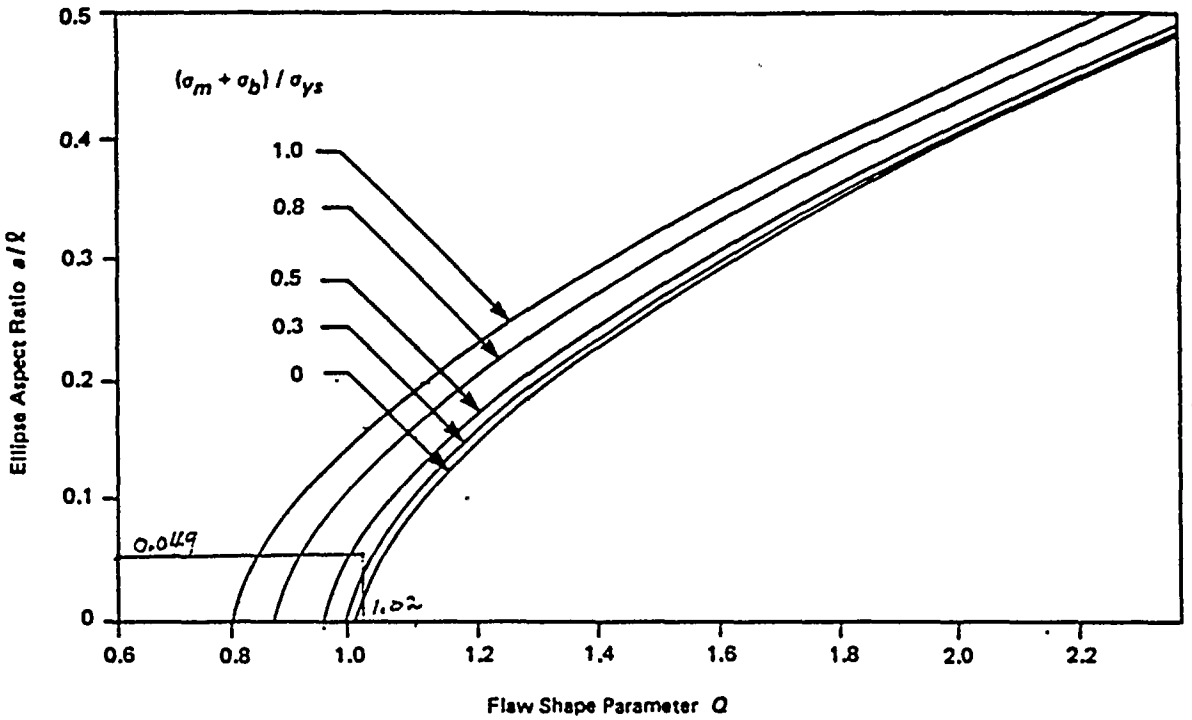

(a) Surface Flaw (b) Subsurface Flaw

σ_{ys} = specified minimum yield strength
ℓ = major axis of ellipse circumscribing the flaw

FIG. A-3300-1 SHAPE FACTORS FOR FLAW MODEL

Prepared by: J. E. [illegible] 4-26-89
Checked by: [illegible] 4/28/89
File No. RGE-04Q-300
Page 8 of 13

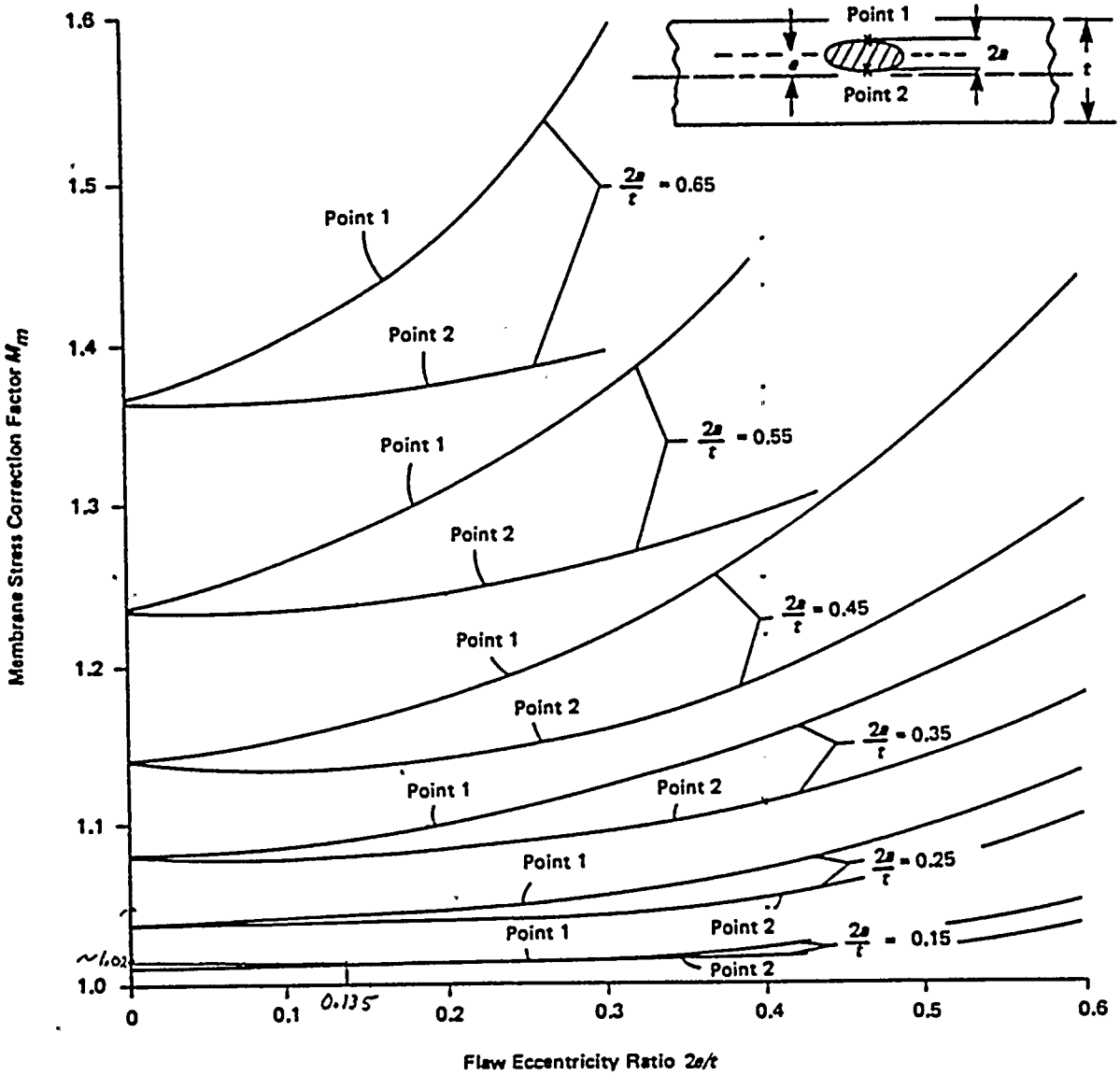

t = wall thickness
e = eccentricity
Point 1 = outer extreme of the minor diameter of ellipse (closer to surface)
Point 2 = inner extreme of the minor diameter of ellipse (further from surface)

FIG. A-3300-2 MEMBRANE STRESS CORRECTION FACTOR FOR SUBSURFACE FLAWS

Prepared by: J.F. Jan 26-89
Checked by: 4/26/89
File No. RGE-040-300
Page 9 of 13

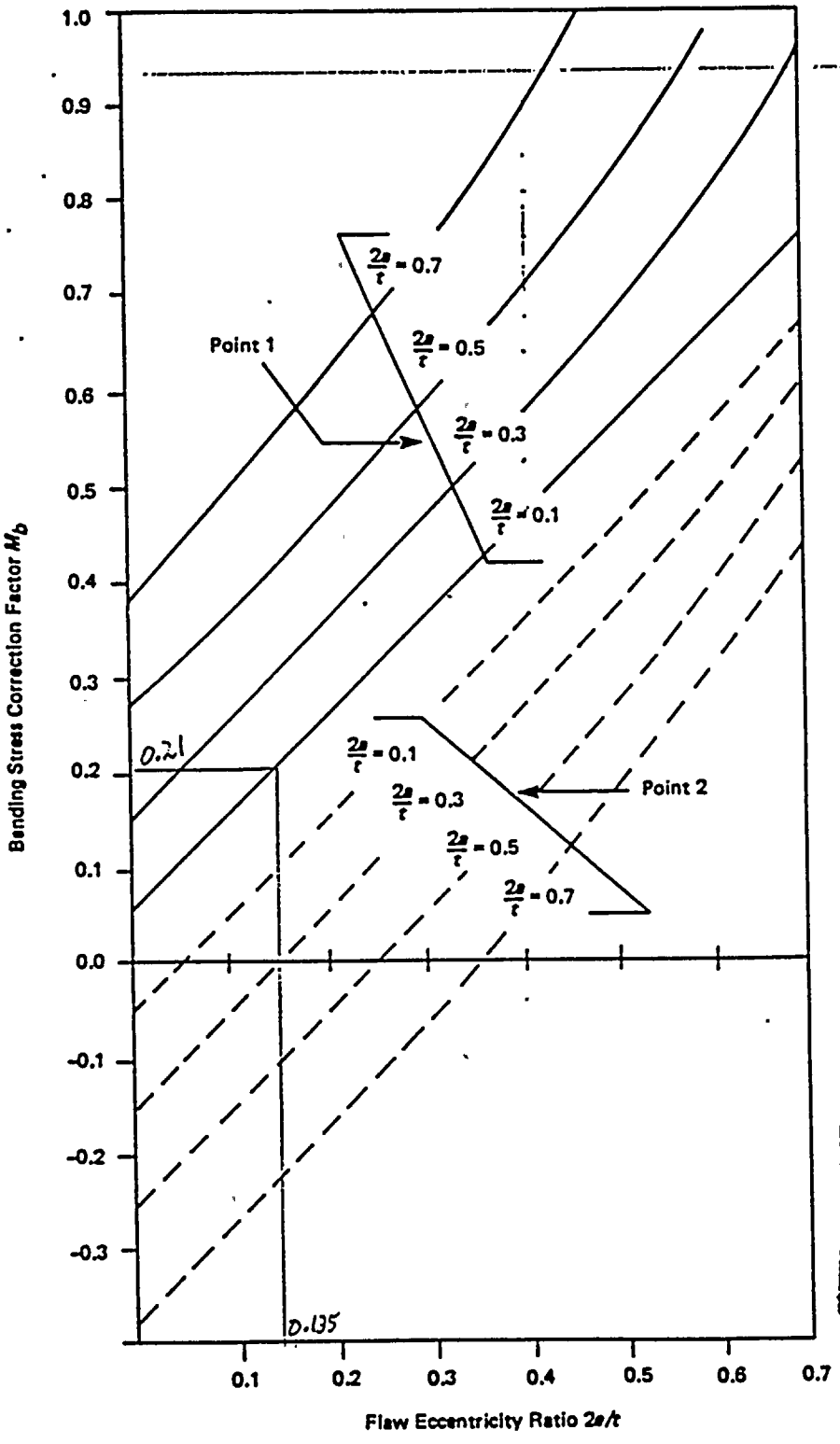

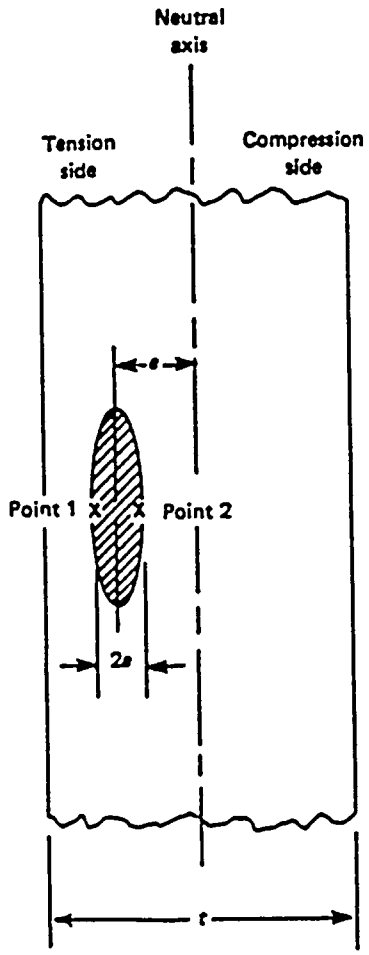

GENERAL NOTE:
If the flaw center line is on the compressive side of the neutral axis, the sign of σ_b should be negative.

Prepared by: [illegible] 4-26-9[illegible]
Checked by: [illegible]
File No. RFE-040[illegible]300
Page 10 of 13

FIG. A-3300-4 BENDING STRESS CORRECTION FACTOR FOR SUBSURFACE FLAWS
(For Definitions of Nomenclature, See Fig. A-3300-2)

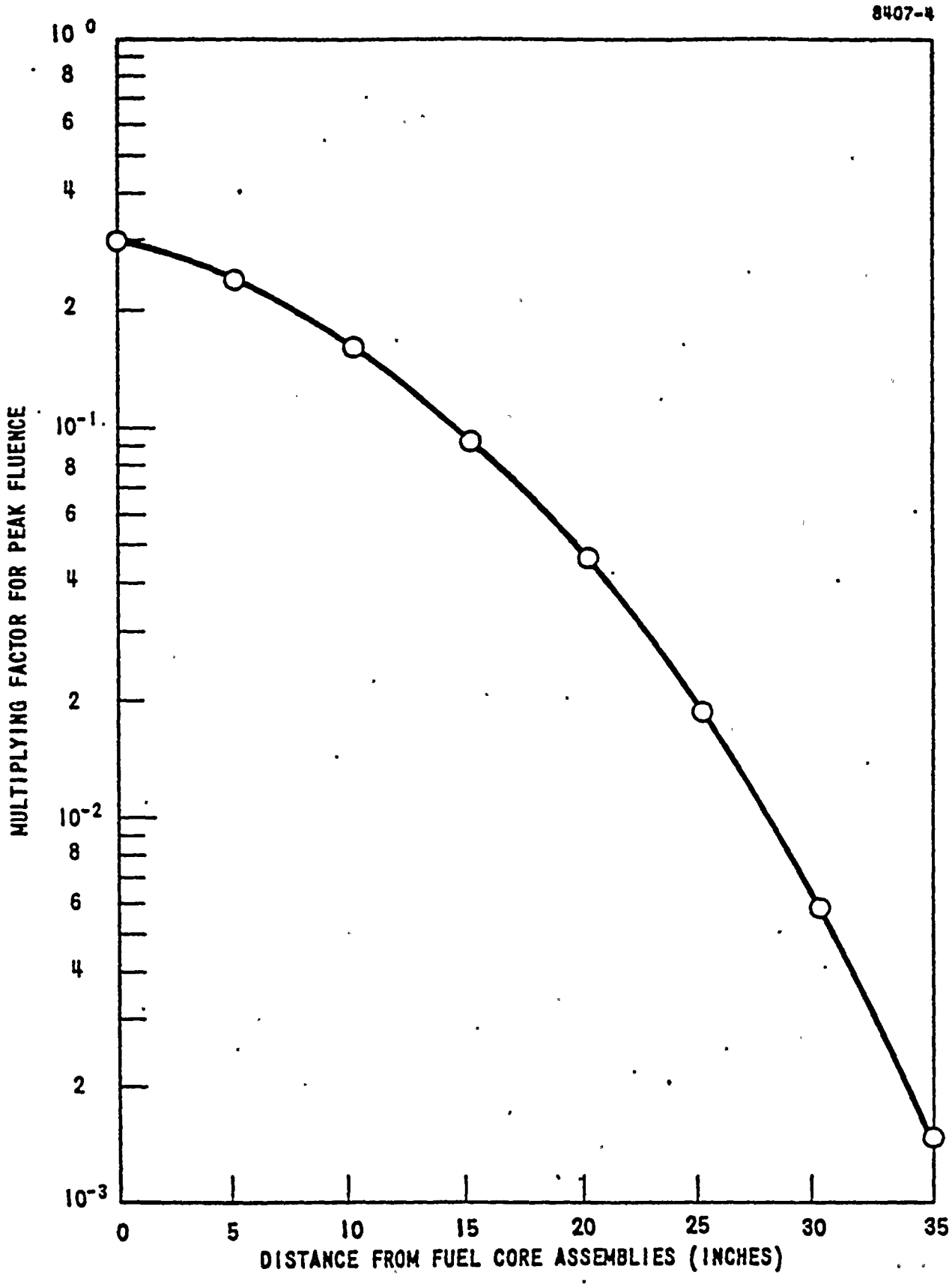

Figure 2-3. Distance Versus Multiplying Factor for Peak Fluence [8]

Prepared by: T. F. Kopp 6-26-87
Checked by: 6/26/89
File No. RFE-040-26
Page 11 of 13

TABLE 2-8
TRANSIENTS VS TEMPERATURES [7]

TRANSIENTS	COLD LEG TEMP RANGE FOR CLOSURE HD, BELTLINE, LOWER HD		HOT LEG TEMP RANGE FOR OUTLET NOZZLE	
	LOW (1) (°F)	HIGH (°F)	LOW (1) (°F)	HIGH (°F)
Heatup (2) - Cooldown	70	547	70	547
Plant Loading & Unloading	541	547	547	607
Small Step Load Decrease	539	555	599	612
Small Step Load Increase	527	543	599	615
Large Step Load Decrease	529	554	528	612
Loss of Load	541	575	544	633
Loss of Power	539	553	583	627
Loss of Flow	497	541	492	613
Reactor Trip From Full Power	531	544	529	607
Turbine Roll	475	550	475	550
Steady State Fluctuations	538	544	604	610
Cold Hydro (2)	70	70	70	70
Hot Hydro (2)	50	400	50	400

NOTE (1) : Use the lower temperature for K_{IR} curve comparison; higher limits are for reference only.

NOTE (2) : These transients are structured to ensure compliance with Appendix G.

Prepared by: J. E. Campbell 4-26-89
Checked by: [illegible] 4/26/89
File No. RTE-OPR-300
Page 12 of 13

TABLE 2-9

TRANSIENTS CONSIDERED IN SUBCRITICAL CRACK GROWTH RATE ANALYSES FOR PRESSURIZER SURGE AND ACCUMULATOR LINES (REFERENCE ~~8~~ 197)

	Operating Cycle	Occurrences in 40 yr. Design Life
1.	Startup and Shutdown	200
2.	Large Step Decrease in Load (with steam dump)	200
3.	Loss of Load (without immediate turbine or reactor trip)	80
4.	Loss of Power (blockout with natural circulation in Reactor Coolant System)	40
5.	Loss of Flow (partial loss of flow, one pump only)	80
6.	Reactor Trip from Full Power	400
7.	Hydrostatic Test (before initial startup, and post operation)	55
8.	High Head Safety Injection	50
		1105

Assume 1200 Significant Cycles in 40 yr. Design Life (30 cycles/yr.)

Prepared by: [signature] 4-26-89
Checked by: [signature] 4/26/89
File No. RGE-040-000
Page 13 of 13